Original Article

Club cell secretory protein 16 promotes cell proliferation and inhibits inflammation and pyroptosis in response to particulate matter 2.5-induced epithelial damage in asthmatic mice

Jinle Lin[1,2#], Xiaowen Chen[1,3,4#], Yuehua Chen[1#], Xiaobing Zeng[5], Fang Wang[1,3], Shaohua Luo[1], Lei Jiang[1], Wenxue Hu[1], Xiaolong Liu[1], Jing Zhang[1], Jian Wu[1]

[1]Second Department of Elderly Respiratory, Guangdong Provincial People's Hospital (Guangdong Academy of Medical Sciences), Southern Medical University, and Guangdong Provincial Institute of Geriatrics, Guangzhou, China; [2]Department of Emergency Medicine, People's Hospital of Shenzhen Baoan District, The Second Affiliated Hospital of Shenzhen University, Shenzhen, China; [3]School of Medicine, South China University of Technology, Guangzhou, China; [4]Beijing Tsinghua Changgung Hospital, Tsinghua University, Beijing, China; [5]Center Lab of Longhua Branch and Department of Infectious Disease, Shenzhen People's Hospital (The Second Clinical Medical College, Jinan University, The First Affiliated Hospital, Southern University of Science and Technology), Shenzhen, China

Contributions: (I) Conception and design: J Lin, X Chen, Y Chen, J Wu; (II) Administrative support: J Lin, X Chen; (III) Provision of study materials or patients: J Lin, X Chen, Y Chen; (IV) Collection and assembly of data: J Lin, X Chen, Y Chen, S Luo, X Zeng, F Wang, L Jiang, W Hu, X Liu, J Zhang; (V) Data analysis and interpretation: J Lin, X Chen, Y Chen; (VI) Manuscript writing: All authors; (VII) Final approval of manuscript: All authors.

[#]These authors contributed equally to this work as co-first authors.

Correspondence to: Dr. Jian Wu, MD, PhD. Second Department of Elderly Respiratory, Guangdong Provincial People's Hospital (Guangdong Academy of Medical Sciences), Southern Medical University, and Guangdong Provincial Institute of Geriatrics, No. 106 Zhongshan 2nd Road, Guangzhou 510080, China. Email: sywujian@scut.edu.cn.

Background: Club cell secretory protein 16 (CC16) has protective roles in airway diseases, including anti-inflammatory, immunomodulatory, and antioxidant functions. This study investigates CC16's potential to repair lung injury from particulate matter 2.5 ($PM_{2.5}$) exposure in asthmatic mice.

Methods: In an ovalbumin (OVA)-induced asthma model, 6-week-old male C57BL/6J mice were exposed to $PM_{2.5}$ for 24 hours and then treated with CC16. We conducted arterial blood gas analysis, lung function tests, histopathology, and immunohistochemical (IHC) staining. The BEAS-2B cell line was exposed to $PM_{2.5}$ for 24 hours and then treated with CC16. Tissues were analyzed by hematoxylin and eosin (HE) staining, electron, and IHC microscopy. The expression of indicators related to inflammation and pyroptosis was also detected and explored by performing RNA sequencing (RNA-seq).

Results: Upon OVA-sensitized asthmatic mice's exposure to $PM_{2.5}$, CC16 therapy reversed lung tissue pathology, corrected acidosis in respiratory gases, and normalized airway constriction. Decreased CC16 also bolstered cellular growth, inhibited $PM_{2.5}$-mediated pyroptosis, and downregulated the expression of inflammatory cytokines and pyroptosis markers at both protein and RNA levels. Transcriptome profiling showed that CC16 modulated the expression of genes linked to inflammatory adhesion, suppressing them, and upregulated those related to proliferation, particularly E-twenty-six-1 (*ETS1*).

Conclusions: CC16 efficiently remedies airway epithelial cells (AECs) harm caused by $PM_{2.5}$ in asthmatic mice, fostering cellular multiplication and suppressing pyroptosis and inflammation. Our findings imply CC16's potential as a promising therapeutic option for addressing future health threats stemming from $PM_{2.5}$ exposure.

Keywords: Club cell secretory protein 16 (CC16); inflammation; pyroptosis; particulate matter 2.5 ($PM_{2.5}$); asthma

Submitted Aug 22, 2024. Accepted for publication Dec 20, 2024. Published online Feb 27, 2025. This article was

updated on July 02, 2025.
The original version was available at: https://dx.doi.org/10.21037/jtd-24-1371
doi: 10.21037/jtd-24-1371

Introduction

Particulate matter 2.5 ($PM_{2.5}$) consists of tiny solid and liquid particles with a diameter of less than 2.5 μm suspended in the air (1,2). High concentrations of $PM_{2.5}$ are known to increase both the incidence and severity of asthma. This condition often involves damage to airway epithelial cells (AECs), which are crucial for maintaining respiratory tract defense and homeostasis. Epithelial dysfunction is hypothesized to be a central mechanism in the pathogenesis of asthma (3).

$PM_{2.5}$ exacerbates asthmatic inflammation and triggers pyroptosis, a form of programmed cell death (4,5). The activation of the nucleotide-binding oligomerization domain-like receptor family pyrin domain containing 3 (NLRP3) inflammasome leads to the release of proinflammatory cytokines interleukin-1β (IL-1β) and IL-18, as well as gasdermin D-induced cell swelling and membrane rupture, culminating in pyroptotic cell death. Elevated levels of NLRP3 and IL-1β have been conducted in the sputum of non-smoking asthma patients (6). Moreover, $PM_{2.5}$ exacerbates lung inflammation and enhances NLRP3 expression. Inhibition of NLRP3 with MCC950, caspase-1 inhibition with Ac-YVAD-CHO, and neutralization of IL-1β have been all proven effective in reducing asthmatic inflammation (7).

Club cell secretory protein 16 (CC16), a member of the secretoglobin superfamily primarily secreted by AECs, exhibits anti-inflammatory and immunoregulatory functions (8,9). Our previous clinical study indicated that a sudden rise in serum CC16 levels in critically ill patients may be associated with secondary acute respiratory distress syndrome (ARDS), with subsequent normalization of CC16 levels reflecting a favorable prognosis (10). Further research has highlighted that the CC16 inhibits toll-like receptor 4 (TLR4)/nuclear factor-κB (NF-κB) inflammatory pathways *in vitro* (11). Studies on lipopolysaccharide (LPS) and bacterial-induced lung injury in mice have demonstrated that extracellular vesicle-associated CC16 could serve as a potential therapeutic agent for acute lung injury (ALI) by mitigating inflammatory and DNA damage responses through reduced NF-κB signaling (12). Epidemiological studies have also reported decreased serum CC16 levels in asthma patients (13). The CC16 A38G polymorphism may contribute to the development of late-onset asthma (14). However, the mechanisms by which CC16 repairs damaged airway epithelium in asthma remain unclear. Previous findings suggest that CC16 has reparative properties in an AEC model exposed to high concentrations of $PM_{2.5}$ for a short duration. Therefore, further investigation into the repair mechanisms and effects of CC16 in models of short-term $PM_{2.5}$ exposure is warranted.

This study aims to explore the repair mechanisms of CC16 in $PM_{2.5}$-induced lung injury using an asthma animal model and the human bronchial epithelial (BEAS-2B) cell line. We present this article in accordance with the ARRIVE reporting checklist (available at https://jtd.amegroups.com/article/view/10.21037/jtd-24-1371/rc) (15).

Highlight box

Key findings

- The study found that club cell secretory protein 16 (CC16) treatment effectively improved lung damage caused by particulate matter 2.5 ($PM_{2.5}$) exposure in asthmatic mice, including alleviating lung tissue pathology, correcting respiratory acidosis, and normalizing airway constriction. CC16 inhibited inflammation and pyroptosis, promoted cellular growth, and modulated gene expression related to inflammation and proliferation, notably upregulating E-twenty-six-1. These findings suggest that CC16 has potential as a therapeutic option for addressing health issues arising from $PM_{2.5}$ exposure.

What is known and what is new?

- CC16 has protective roles in airway diseases and $PM_{2.5}$ exposure-induced lung injury and inflammation.
- This study shows CC16 alleviates lung damage in asthmatic mice exposed to $PM_{2.5}$ by reducing inflammation and pyroptosis, promoting cellular growth, and altering gene expression related to inflammation and proliferation.

What is the implication, and what should change now?

- CC16 shows that promise as a therapeutic option for protecting against lung damage from $PM_{2.5}$ exposure, potentially benefiting patients with asthma and other respiratory conditions.
- Further research is needed to confirm CC16's efficacy and safety in clinical settings. Development of targeted therapies based on CC16's mechanism could advance treatment strategies for $PM_{2.5}$-related lung injuries.

Methods

The following experimental methods are a brief description. For details, see Appendix 1.

Collection of $PM_{2.5}$ and sample preparation

$PM_{2.5}$ samples were collected in August 2020 from the rooftops of the Guangzhou Institute of Geochemistry, Chinese Academy of Sciences (located 100 m from the motorway) using high-volume air samplers (Thermo Fisher Scientific, Waltham, MA, USA). Quartz fiber filter membranes (20×25 cm^2) loaded with $PM_{2.5}$ were washed, filtered, centrifuged, and freeze-dried to obtain $PM_{2.5}$ powder. In the experiment, this powder was dissolved in normal saline or phosphate-buffered saline (PBS). Ion chromatography and water-soluble total organic carbon were respectively analyzed by using inductively coupled plasma mass spectrometry (Thermo Finnegan, San Jose, CA, USA), Organic carbon/elemental carbon analyzer (Desert Research Institute, Reno, NV, USA) (date in Table S1).

Animal model and ethics statements

Male C57BL/6J mice were randomly assigned to six groups (n=20 per group) and subjected to different treatments. The study protocols were approved by the Research Animal Care Committee of Southern Medical University. The mice were randomly assigned to the following six groups of 20 each:

(I) Control group: the mice were sensitized to be injected with neutral saline via the intraperitoneal route on days 1, 7, and 14. During days 21–30, the mice were exposed to neutral saline via ultrasonic nebulizers (402AI, Jiangsu Yuyue Medical Equipment & Supply Co., Ltd., Zhenjiang, China).

(II) Asthma group: the mice were sensitized to be injected with 1 mg ovalbumin (OVA) (Sigma, St. Louis, MO, USA) mixed with 100 mg alum (Sigma) intraperitoneally on days 1, 7, and 14. During days 21–27, the mice were exposed to 1% OVA aerosol with 8-mL saline solution through ultrasonic nebulizers for 30-min daily.

(III) $PM_{2.5}$ (24 h) group: the OVA-induced mice were exposed to 2 mg $PM_{2.5}$ in 8 mL nebulizer solution (0.25 mg/mL) through ultrasonic nebulizers for a 2-h-course on day 28.

(IV) $PM_{2.5}$ (48 h) group: the OVA-induced mice were exposed to 2 mg $PM_{2.5}$ in 8 mL nebulizer solution (0.25 mg/mL) through ultrasonic nebulizers for a 2 hours course on day 28 and then exposed to neutral saline on day 29.

(V) $PM_{2.5}$ + CC16 (24 h) group: the OVA-induced mice were exposed to 2 mg $PM_{2.5}$ in 8 mL nebulizer solution (0.25 mg/mL) through compression atomizers for a 2-h-course on day 28 and then exposed to 2 mg CC16 in 8 mL nebulizer solution (0.25 mg/mL) (USCN Sciences Co., Wuhan, China) with 8 mL saline solution through ultrasonic nebulizers for a 2-h-course on day 29.

(VI) $PM_{2.5}$ + CC16 (48 h) group: the OVA-induced mice were exposed to 2 mg $PM_{2.5}$ in 8 mL nebulizer solution (0.25 mg/mL) through compression atomizers for a 2-h-course on day 28 and then exposed to 2 mg CC16 in 8 mL nebulizer solution (0.25 mg/mL) through ultrasonic nebulizer for a 2-h-course on days 29 and 30.

Normal mice have a minute ventilation volume of 300 mL, with a settling rate of $PM_{2.5}$ in the lungs at 6.67%. The nebulizer efficiency requires an oxygen flow rate of 3 mL/min. $PM_{2.5}$ is dissolved in physiological saline at a concentration of 2 mg in 8 mL, and continuously atomized for 2 hours. The exposure level of $PM_{2.5}$ in this animal experiment is 62 μg per cubic meter, equivalent to 200 μg per mL in cell experiments. The intervention concentration of CC16 in animal experiments is 0.3225 μg per cubic meter, approximately equal to 1 mL. The next day, the mice were anesthetized with pentobarbital (1.5% pentobarbital sodium, 0.1 mL/20 g) and subjected to exsanguination. The protocol used for this experiment is illustrated in *Figure 1*.

The study was conducted in accordance with the Guidelines for the Care and Use of Laboratory Animals issued by the Ministry of Science and Technology of the People's Republic of China (the National Standard GB/T 35892-2018). Additionally, the research was approved by the Ethics Committee of Southern Medical University (approval No. BYL20231202).

Artery blood gas

Four mice were anesthetized with pentobarbital (40 mg/kg) to evaluate the lung oxygenation status. An arterial blood gas needle (Radiometer, Copenhagen, Denmark) was placed with a 24-gauge needle (Introcan™-W) in the abdominal aorta when the abdomen opened. Then, 1.5–2 mL of

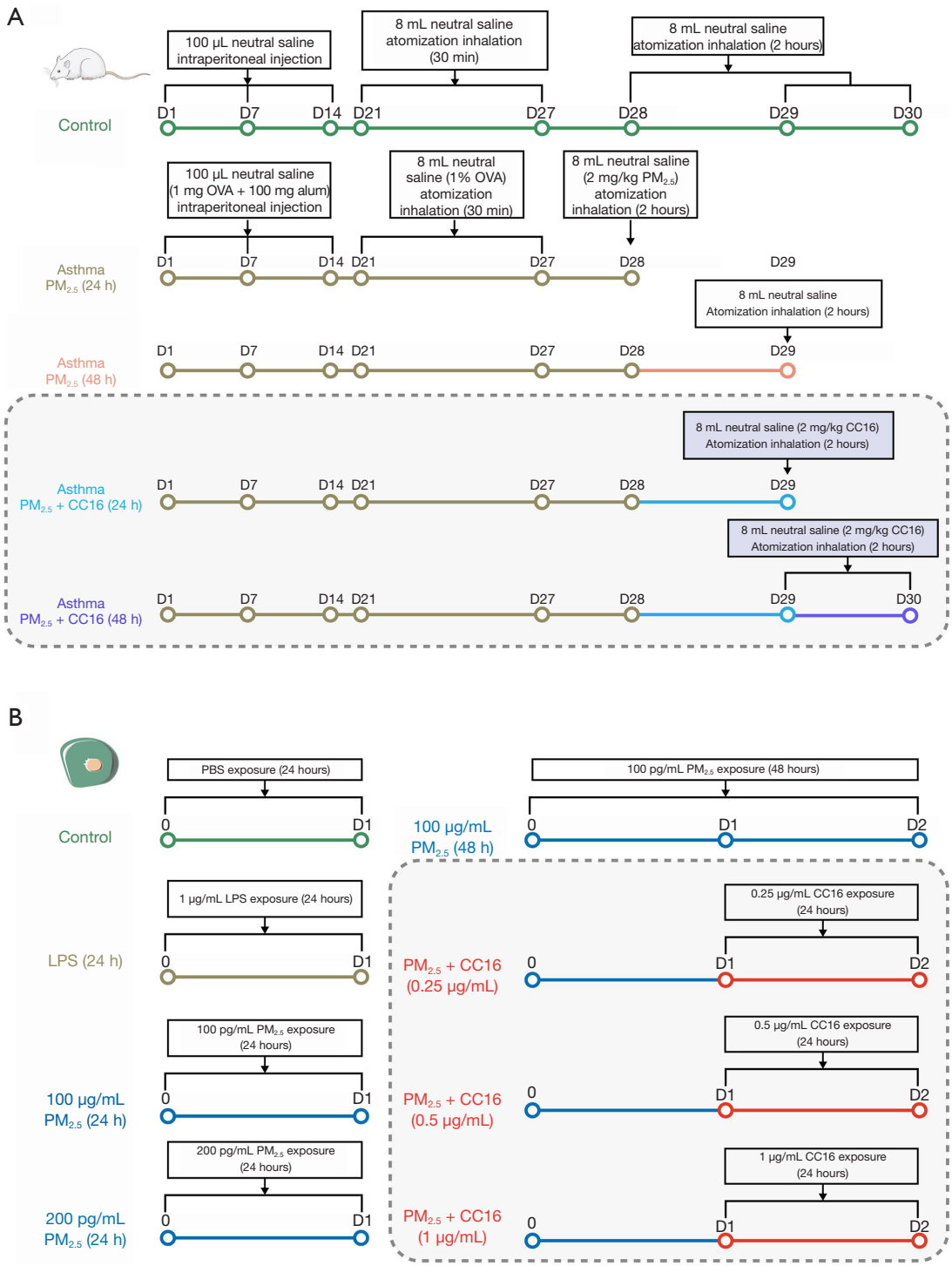

Figure 1 The mouse asthma model was induced via the intraperitoneal injection and atomization of OVA until day 27. $PM_{2.5}$ (2 mg/kg) was administrated to the mice in the $PM_{2.5}$ group on day 28. CC16 (2 mg/kg) was administered to the mice in the $PM_{2.5}$ + CC16 group on day 28 after exposure to $PM_{2.5}$. BEAS-2B cells were incubated with (100 and 200 μg/mL) $PM_{2.5}$ with 24 and 48 h, CC16 (0.25, 0.5, and 1 μg/mL) was administered to the cell medium after the cells were exposed to 100 μg/mL $PM_{2.5}$ for 24 hours. (A) Mouse model experimental protocol. (B) $PM_{2.5}$/CC16 exposure group comparisons. D, day; OVA, ovalbumin; $PM_{2.5}$, particulate matter 2.5; CC16, club cell secretory protein 16; PBS, phosphate-buffered saline; LPS, lipopolysaccharide.

arterial blood was analyzed with a radiometer (ABL825, Radiometer). Next, we determined the partial pressures of oxygen (PaO_2), partial pressures of carbon dioxide ($PaCO_2$), hydrogen potential (pH) of arterial blood gases, and anion gap (AG).

Lung function

Five mice were assessed for their airway responsiveness to methacholine. The methacholine and allergen challenge tests were conducted using the FinePointe RC (Buxco Research Systems, Data Sciences International, New Brighton, MN, USA). After anesthetizing with sevoflurane for 7 seconds, the mice were placed in the mechanically ventilated system with increasing doses of methacholine (TCI, Shanghai, China) and sequentially nebulized. Methacholine is a bronchoconstrictor-inducing airway contraction used to nebulize at varying doses in 10 µL volume, ranging from 0 to 50 mg/mL. For each dose, lung resistance was measured and computed over 3 min. The respiratory data were acquired and presented with the FinePointe station.

Histopathology, bronchoalveolar lavage (BAL), and immunohistochemical (IHC) staining

For scoring analysis, the sections were stained with hematoxylin and eosin (HE) and assessed for injury severity using the Smith Lung Injury Scoring System. Following anesthesia, the trachea of the mice was carefully isolated from the neck region, and the chest cavity was subsequently opened. The left lung was ligated, and 0.2 mL of PBS was gradually administered into the left lung via an air tube using a 1 mL syringe. This procedure was repeated three times to ensure thorough aspiration, resulting in a BAL recovery rate exceeding 80%. The concentration of IL-1β in the BAL was then quantified using an enzyme-linked immunosorbent assay (ELISA), following the manufacturer's protocol. The sections were then subjected to IHC staining using primary antibodies against TLR4 (1:100, Abcam, Cambridge, UK), anti-phospho-NF-κB (1:150, Abcam), caspase-1 (1:500, Bioss, Beijing, China), and IL-1β (1:100, Abcam). IHC images were captured using a light microscope at ×200 magnification and analyzed with ImageJ to quantify the positive staining percentage.

BEAS-2B cell sourcing, exposure to $PM_{2.5}$, and treatment of CC16

BEAS-2B cells were obtained from the Cell Bank of the Chinese Academy of Sciences (Shanghai, China). The cells were cultured in Dulbecco's modified Eagle's medium/F12 (DMEM/F12, Gibco, Grand Island, NY, USA) supplemented with 5% fetal bovine serum (FBS; Gibco) and 1% penicillin-streptomycin. $PM_{2.5}$ was sterilized with 20 min of high-temperature autoclaving. The protocol for generating cell models is illustrated in *Figure 1B*, as follow:

(I) BEAS-2B cells were incubated with $PM_{2.5}$ (100 and 200 µg/mL) in DMEM/F12 medium without FBS for 24 hours;
(II) In the subgroup with $PM_{2.5}$ (100 µg/mL), BEAS-2B cells were first exposed to 100 µg/mL $PM_{2.5}$ for 24 hours and then to 0.25, 0.5, and 1 µg/mL CC16 (R&D Systems, Catalog #: 4218-UT, Minneapolis, MN, USA) administrated to the cell medium for 24 hours.

Cell Counting Kit-8 (CCK-8) assay

The CCK-8 solution (Abcam) was added to the culture medium and incubated for 2 hours following $PM_{2.5}$ or CC16 administration, according to the manufacturer's instructions. Cell viability in each group was assessed using a microplate reader at an optical density of 450 nm.

Cell fluorescence microscopy

Cell viability was assessed by light-sheet microscopy. Propidium iodide (PI; 5 µg/mL; Sigma) was incubated for 10 min in the dark. The types of cell death were assessed using the Annexin V-fluorescein isothiocyanate (FITC)/PI Fluorescence Microscopy Kit (BD Biosciences, San Diego, CA, USA) and Hoechst 33342 (BD Biosciences). The cells were washed twice with PBS and then Annexin V Binding Buffer. The cells were then stained at room temperature with Hoechst 33342 (diluted 1:20) for 10 min, with Annexin V-FITC (diluted 1:10) for 10 min, and with PI (5 µg/mL) for 5 min. The stained cell climbing slice was fixed with antifade mounting medium (BOSTER, Co., Ltd., Pleasanton, CA, USA). The slice was observed under a confocal fluorescence microscope (Nikon, Tokyo, Japan) at 405, 488, and 640 nm excitation wavelength.

Table 1 Primers of PCR target protein genes

Target gene	Forward primer (5'-3')	Reverse primer (5'-3')
Caspase-1	CATGGGTGAAGATAATGTTTCTTGG	GCATCTGCGCTCTACCATCT
Gasdermin D	TCTGCCCTCAACACTTCTGG	TGCAGCCACAAATAACTCAGC
IL-1β	AGAAGTACCTGAGCTCGCCA	CTGGAAGGAGCACTTCATCTGT
GADPH	GAAGATGGTGATGGGATTTC	GAAGGTGAAGGTCGGAGTC

PCR, polymerase chain reaction; IL-1β, interleukin-1β; GADPH, glyceraldehyde-3-phosphate dehydrogenase.

Scanning electron microscopy

The slides of BEAS-2B cells after treatment with $PM_{2.5}$ or CC16 were dehydrated in a gradient series of ethanol (30%, 40%, 50%, 60%, 70%, 80%, 90%, and 100%) and critical point CO_2. The sample was then adhered to a stage with double-sided conductive tape, sprayed with an ion sputter, and observed and photographed with an electron microscope (Zeiss Merlin, Oberkochen, Germany).

Western blotting

Proteins from lung tissue samples and cell lysates were separated by sodium dodecyl sulfate-polyacrylamide gel electrophoresis (SDS-PAGE). Western blot analysis was performed using primary antibodies against TLR4, NF-κB, polyclonal anti-NF-κB, caspase-3, NLRP3, caspase-1, IL-1β, gasdermin D, high mobility group box 1 (HMGB1), E-twenty-six-1 (ETS1), and β-actin. The grayscale values of the Western blot strips were quantified using ImageJ.

Real-time polymerase chain reaction (PCR)

Real-time PCR was performed using the QuantiFast SYBR Green PCR Kit (Invitrogen, Carlsbad, CA, USA) on the Roche LightCycler 480 II system. For details, see Appendix 1. The primer sequences are listed in *Table 1*.

Database construction, analysis, and validation based on transcriptome data

BEAS-2B cells treated with either CC16 or $PM_{2.5}$ were subjected to RNA extraction using TRIzol's protocol, followed by RNA quantification using an ELISA at 562 nm. The reaction solution was prepared on ice per the Total RNA sequencing (RNA-seq) (H/M/R) Library Prep Kit instructions. Subsequently, the RNA samples were placed in a PCR reactor, and RNase H and DNase I digestion reactions were performed to obtain a 5 μG total RNA sample. The ribosomal deleted RNA was purified through VAHTS RNA Clean Beads, followed by the synthesis of complementary DNA (cDNA) based on the size of the inserted fragment. The cDNA synthesis reaction solution was prepared in a PCR reaction tube, and two synthesis reactions were performed. The RmRNA seq library underwent 100 bp double-ended sequencing using HiSeq2000. The Fatsqc tool is utilized for quality control of messenger RNA (mRNA) sequencing data, with the additional step of pruning low-quality bases. The RNA-seq data is subsequently mapped to the Human Genome (hg19) via TopHat (version 2.1.1), with a maximum allowance of two mismatches. The gene expression level is then calculated using Cufflinks, with default parameters being employed. Finally, Gene Ontology (GO) analysis is conducted using DAVID. The Western blot technique is utilized to verify the protein expression of genes that have undergone screening.

Statistical analysis

Data were presented as the mean ± standard deviation. Statistical analyses were performed using SPSS version 14.0 (SPSS Inc., Chicago, IL, USA). The Student's *t*-test was used to compare differences between the two groups. One-way analysis of variance (ANOVA) followed by Bonferroni's post-hoc test was employed for comparisons among multiple experimental groups. A P value of <0.05 was considered statistically significant.

Results

Lung tissue damage, respiratory acidosis, and increased airway resistance in asthmatic mice due to $PM_{2.5}$ exposure

Arterial blood gas analysis revealed a decline in PaO_2 following 24-hour exposure to $PM_{2.5}$, while a 48-hour exposure period resulted in a notable decrease in pH and

an increase in $PaCO_2$, as compared to the control group mice (refer to *Figure 2A*). Pulmonary function assessments indicated a statistically significant elevation in airway resistance parameters, specifically specific airway resistance (sRaw) and peak inspiratory flow (PIF), among mice exposed to $PM_{2.5}$ (depicted in *Figure 2B*). These findings suggest heightened airway resistance, airway hyperresponsiveness, and respiratory distress. Additionally, exposure to $PM_{2.5}$ exacerbated the manifestation of airway inflammation in asthmatic mice, as evident from *Figure 2C,2D*. The mortality rate of mice subjected to treatment for a duration of 48 hours is similar.

IHC and western blot in $PM_{2.5}$ exposed asthmatic mice

IHC staining has demonstrated that exposure to $PM_{2.5}$ significantly stimulates the expression of TLR4, phosphorylated NF-κB, caspase-1, and IL-1β in the lung tissue of mice, as depicted in *Figure 3A*. Additionally, Western blot analysis has confirmed that inflammatory pathways, encompassing TLR4, phosphorylated NF-κB, caspase-3, and NF-κB, along with pyroptosis-related markers such as NLRP3, caspase-1, gasdermin D, and IL-1β, exhibit heightened expression levels subsequent to $PM_{2.5}$ exposure, in comparison to pre-exposure levels, as shown in *Figure 3B*. Notably, these protein levels persist in an upward trend even after 48 hours of exposure to $PM_{2.5}$.

The administration of CC16 relived ALI, respiratory acidosis, and airway distress in asthmatic mice due to $PM_{2.5}$ exposure

The analysis of arterial blood gases revealed marked improvements in blood gas parameters among the mice treated with CC16, as compared to the two other asthma model groups exposed to $PM_{2.5}$ (*Figure 4A*). Notably, there was an elevation in pH and PaO_2 values, accompanied by a reduction in $PaCO_2$, albeit with less pronounced alterations in the AG. Furthermore, pulmonary function assessments demonstrated that CC16 treatment alleviated the $PM_{2.5}$-induced abnormalities in sRaw and PIF (*Figure 4B*). Specifically, a 24-hour treatment with CC16 nearly restored sRaw and PIF to normal levels, whereas a 48-hour treatment fully normalized sRaw. HE staining highlighted that the lung injury caused by $PM_{2.5}$ exposure, which was characterized by inflammation, hemorrhage, and necrosis. Importantly, CC16 treatment mitigated these effects, resulting in a decreased Smith lung injury score (*Figure 4C,4D*).

CC16 resulted in the suppression of increased levels of inflammation and pyroptosis proteins in asthmatic mice exposed to $PM_{2.5}$

The IHC and Western blot analyses have consistently demonstrated that nebulization therapy utilizing CC16 effectively suppresses the expression of inflammatory and pyroptotic signaling proteins within lung tissue. Specifically, in mice administered with CC16 nebulization, a notable decrease was observed in the levels of TLR4, phosphorylated NF-κB, caspase-1, and IL-1β proteins. Furthermore, the expression of NF-κB, NLRP3, gasdermin D, and IL-1β was significantly inhibited, as evidenced in *Figure 5A,5B*.

$PM_{2.5}$ caused pyroptosis and increased activation of inflammatory in BEAS-2B cells

To rigorously examine the consequences of $PM_{2.5}$ exposure, we subjected BEAS-2B cells to stimulation with $PM_{2.5}$ and subsequently performed CCK-8 assays to quantitatively assess their viability, as depicted in *Figure 6A*. Through the utilization of Annexin V-FITC/PI/Hoechst 33342 staining and confocal microscopy, we conclusively identified the occurrence of cell death in these BEAS-2B cells, as evidenced in *Figure 6B*. Furthermore, scanning electron microscopy provided corroborating evidence, revealing that $PM_{2.5}$ exposure compromised the structural integrity of the cell membrane, manifested through phenomena such as membrane perforation, surface damage, and irregular cell morphology, as illustrated in *Figure 6C*.

Drawing upon the foundations laid by previous animal studies, our investigation centered on elucidating the mechanisms of cell pyroptosis and inflammatory protein expression. Western blot analysis indicated that, in comparison to the control group, exposure to $PM_{2.5}$ and LPS triggered the phosphorylation of NF-κB within the inflammatory signaling pathway. Additionally, we observed elevated expression levels of cleaved caspase-3 and HMGB1, alongside significant increases in cleaved caspase-1, cleaved gasdermin D, and IL-1β within the pyroptotic signaling pathway, as depicted in *Figure 7A-7D*. These findings were further supported by elevated RNA transcription levels of caspase-1, gasdermin D, and IL-1β in the $PM_{2.5}$ and LPS

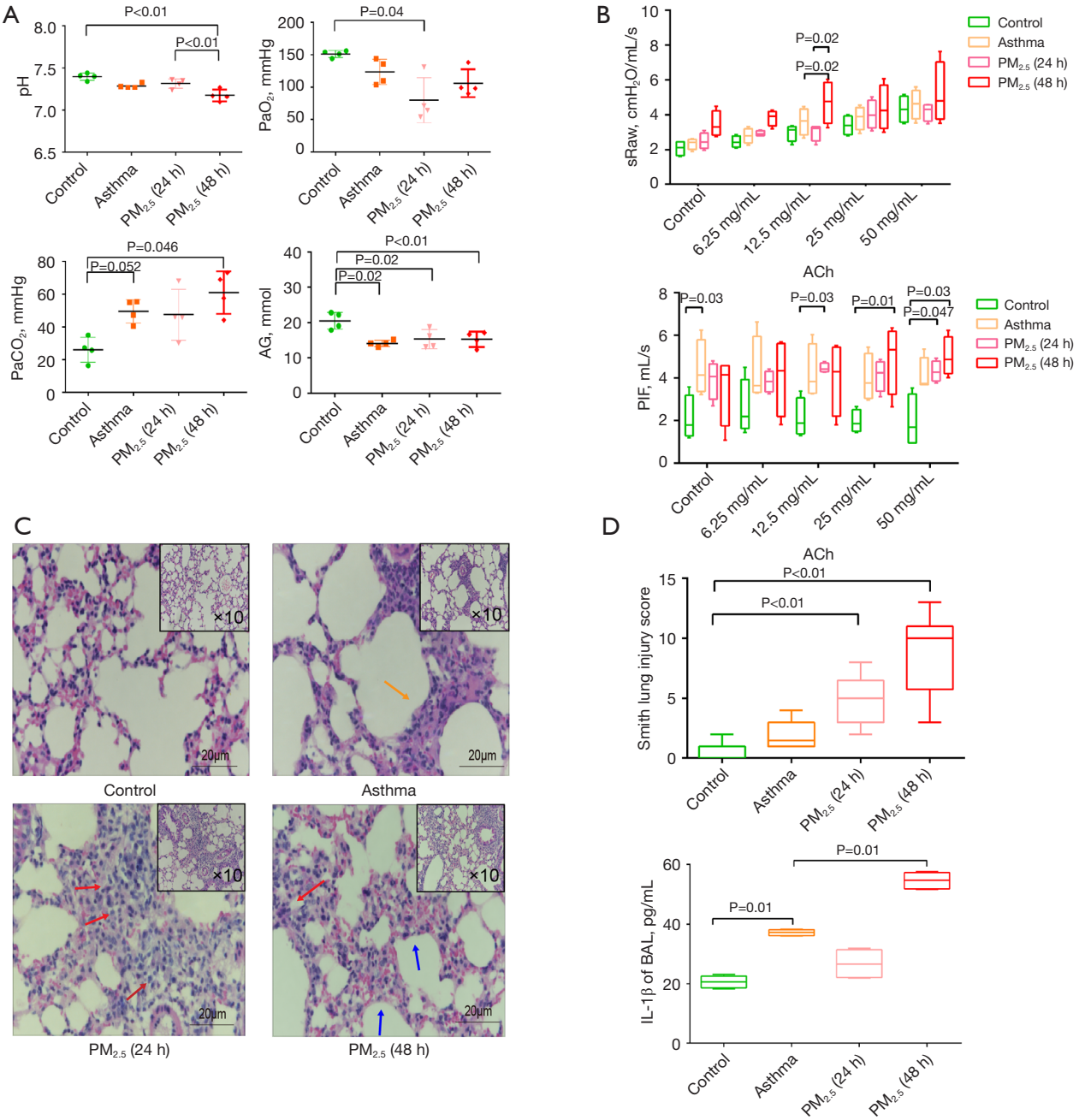

Figure 2 Analysis of OVA induction and exposure to $PM_{2.5}$ on mice. (A) Blood gas. (B) The lung function. (C) HE staining of lung tissue. The red arrows denote the injury of ciliated cells in the trachea; the blue arrows denote infammatory reaction, hemorrhage, and necrosis; the orange arrow suggests eosinophilic infltration of the alveolar epithelial barrier. (D) Injury score in lung tissue and level of IL-1β in BAL (n=4 in each group). pH, hydrogen potential; $PM_{2.5}$, particulate matter 2.5; PaO_2, partial pressures of oxygen; $PaCO_2$, partial pressures of carbon dioxide; AG, anion gap; sRaw, specific airway resistance; ACh, acetylcholine; PIF, peak inspiratory flow; IL-1β, interleukin-1β; BAL, bronchoalveolar lavage; OVA, ovalbumin; HE, hematoxylin and eosin.

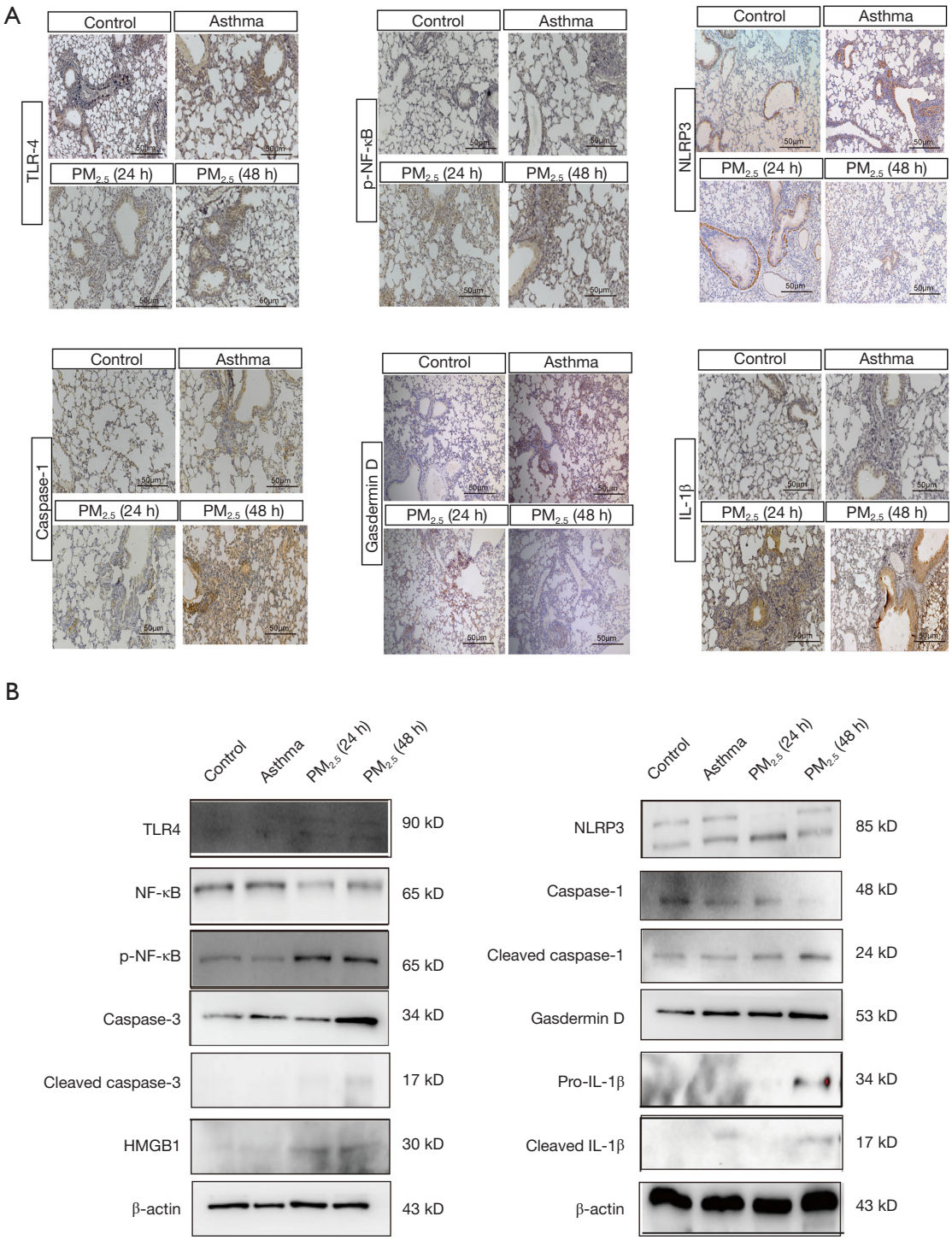

Figure 3 Lung injury induced by OVA and exposure to $PM_{2.5}$. (A) IHC staining (n=10 in each group). (B) Western blot of lung tissue (n=3 in each group). Full-length blots/gels were presented in Figure S1. TLR4, toll-like receptor 4; $PM_{2.5}$, particulate matter 2.5; p-, phospho-; NF-κB, nuclear factor-κB; NLRP3, nucleotide-binding oligomerization domain-like receptor family pyrin domain containing 3; IL-1β, interleukin-1β; HMGB1, high mobility group box 1; OVA, ovalbumin; IHC, immunohistochemical.

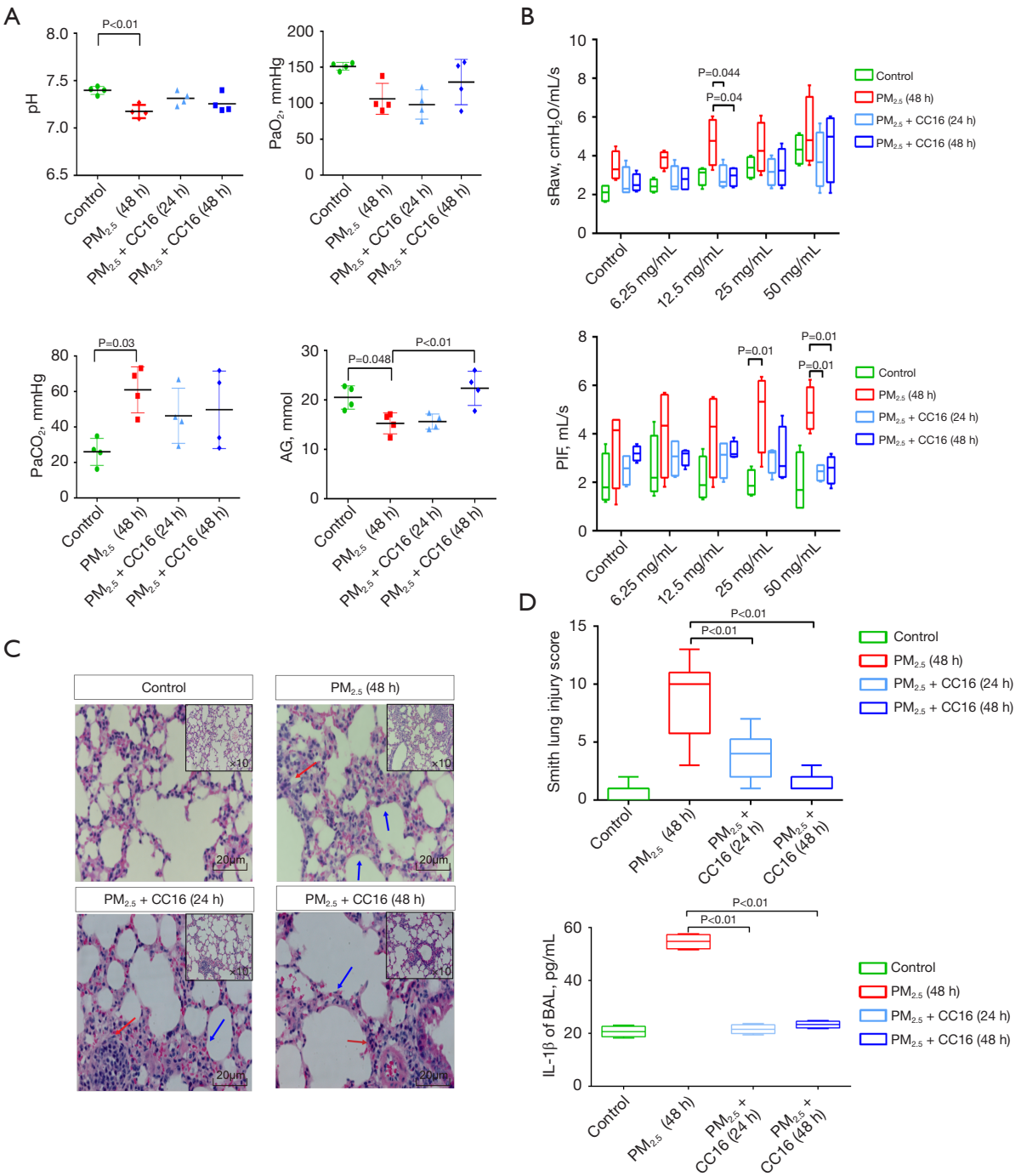

Figure 4 The evaluation of CC16 on mice after exposure to $PM_{2.5}$. (A) Blood gas. (B) lung function. (C) HE staining of lung tissue. The red arrows denote inflammatory reaction, the blue arrows denote repairment of lung tissue. (D) Injury score in lung tissue and level of IL-1β in BAL (n=4 in each group). pH, hydrogen potential; $PM_{2.5}$, particulate matter 2.5; CC16, club cell secretory protein 16; PaO_2, partial pressures of oxygen; $PaCO_2$, partial pressures of carbon dioxide; AG, anion gap; sRaw, specific airway resistance; ACh, acetylcholine; PIF, peak inspiratory flow; IL-1β, interleukin-1β; HE, hematoxylin and eosin; BAL, bronchoalveolar lavage.

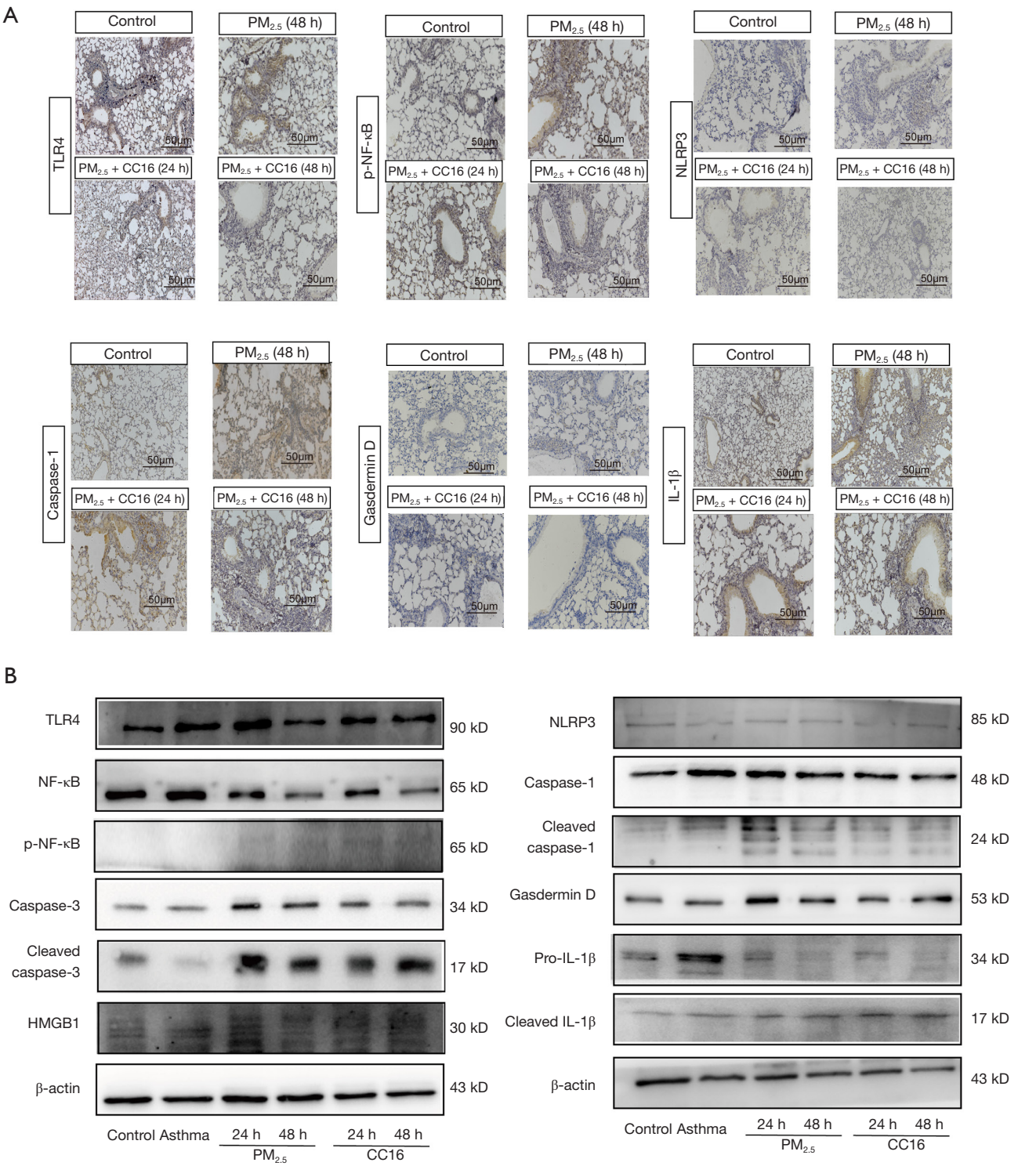

Figure 5 IHC and western blot were used to measure the protein expression levels of CC16-treated mice after exposure to $PM_{2.5}$. (A) IHC staining (n=10 in each group). (B) Western blot of lung tissue (n=3 in each group). Full-length blots/gels were presented in Figure S2. TLR4, toll-like receptor 4; $PM_{2.5}$, particulate matter 2.5; CC16, club cell secretory protein 16; p-, phospho-; NF-κB, nuclear factor-κB; NLRP3, nucleotide-binding oligomerization domain-like receptor family pyrin domain containing 3; IL-1β, interleukin-1β; HMGB1, high mobility group box 1; IHC, immunohistochemical.

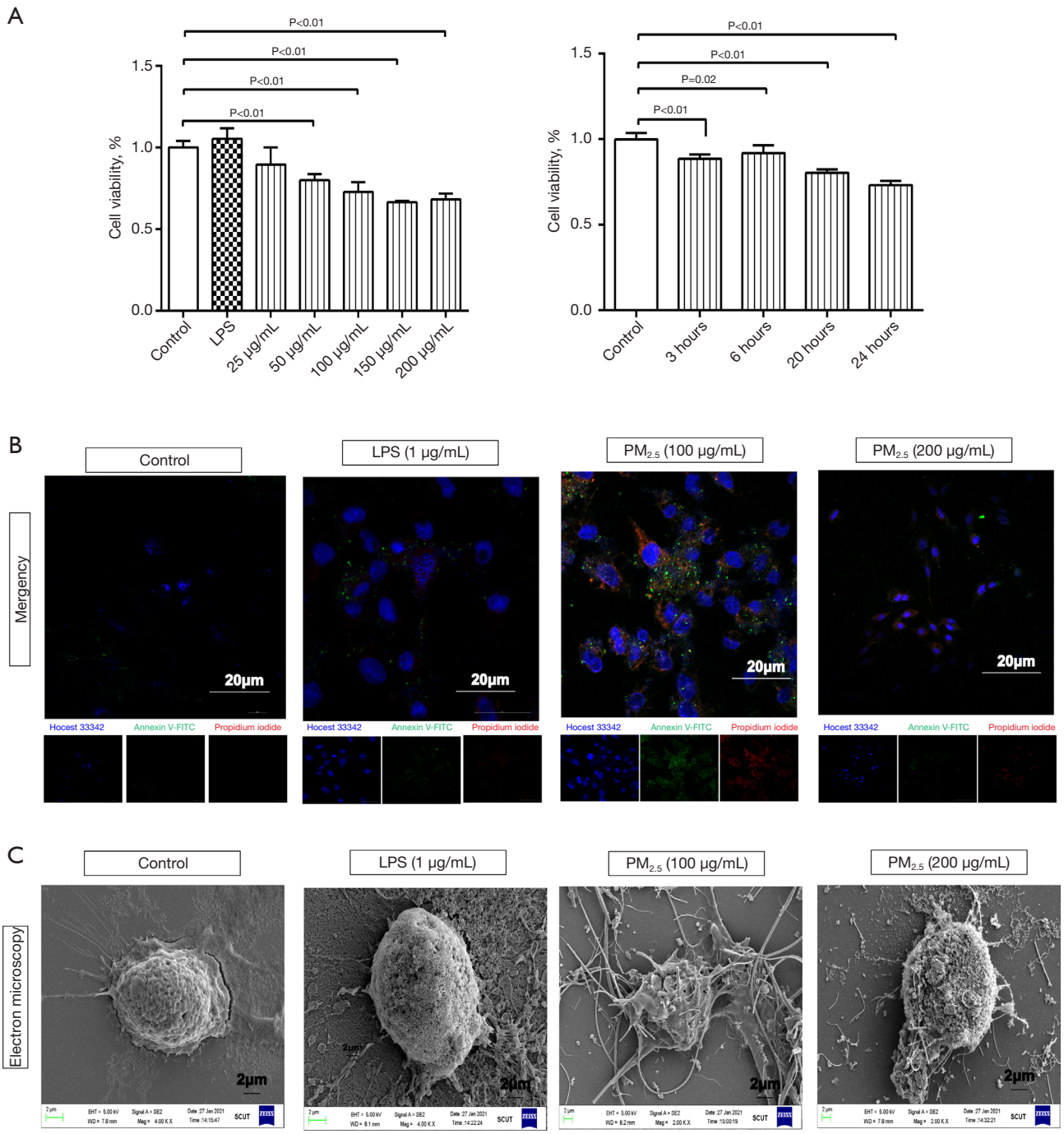

Figure 6 Light microscopy, CCK-8, confocal microscopy, and electron microscopy of the alterations in BEAS-2B cells exposed to $PM_{2.5}$. (A) Cell viability was inferred from CCK-8 analysis. (B) Confocal microscopy, Hocest 33342 staining (blue), Annexin V-FITC (green), PI (red). (C) Electron microscopy. LPS, lipopolysaccharide; $PM_{2.5}$, particulate matter 2.5; EHT, electron high yension; WD, working distance; Mag, magnification; SCUT, South China University of Technology; CCK-8, Cell Counting Kit-8; FITC, fluorescein isothiocyanate; PI, propidium iodide.

exposure groups, relative to the control group, as shown in *Figure 7E*. Collectively, these results underscore the capacity of $PM_{2.5}$ to induce pyroptosis and augment inflammatory activation in BEAS-2B cells.

The administration of CC16 ameliorated in $PM_{2.5}$-induced pyroptosis and inflammation in BEAS-2B cells

To investigate the role of CC16 in mitigating pyroptosis and inflammation, we observed alterations in cell morphology and viability subsequent to treating $PM_{2.5}$-exposed BEAS-2B cells with varying concentrations of CC16. Notably, the proliferation of BEAS-2B cells exposed to $PM_{2.5}$ was contingent upon both the dosage and duration of CC16 treatment, as depicted in *Figure 8A*,*8B*. CC16 treatment effectively mitigated $PM_{2.5}$-induced pyroptosis. Confocal microscopy, coupled with fluorescence staining, illuminated that CC16 facilitated the restoration of the cell membrane. This observation was corroborated by scanning electron microscopy, which showed that surviving cells exhibited smooth and uncompromised cell membranes, devoid of surface protrusions indicative of pyroptosis, and maintained their normal morphology without any discernible deformations (*Figure 8C*). Western blot analysis indicated a significant reduction in the expression of phosphorylated NF-κB, caspase-3, caspase-1, gasdermin D, HMGB1, and IL-1β in the CC16-treated group compared to the $PM_{2.5}$-exposed group (*Figure 9A*,*9B*). Additionally, real-time PCR analysis confirmed that the transcription levels of caspase-1, gasdermin D, and IL-1β were lower in the CC16-treated group than in the $PM_{2.5}$-exposed group (*Figure 9C*). These findings underscore the efficacy of CC16 in suppressing the upregulation of inflammation and pyroptosis signaling pathways triggered by $PM_{2.5}$ exposure.

CC16 regulated genes expression profiles in $PM_{2.5}$-induced alveolar epithelial cells

In this study, a rigorous approach was adopted utilizing principal component analysis (PCA) to evaluate the quantitative reproducibility of differentially expressed genes and ensure statistical robustness in the quantification of cell samples (*Figure 10A*). Exposure to $PM_{2.5}$ resulted in the identification of 1,100 genes that were upregulated and 1,180 genes that were downregulated. Notably, subsequent treatment with CC16 revealed a common upregulation in 37 genes and downregulation in 20 genes (*Figure 10B*,*10C*). Intriguingly, CC16 intervention led to a reversal in expression patterns for 10 genes initially upregulated in the $PM_{2.5}$ group, with a decrease in expression, and for 21 genes initially downregulated in the $PM_{2.5}$ group, with an increase in expression (Table S2). These differentially expressed genes underwent GO enrichment analysis for functional classification and pathway identification. Significantly enriched differentially expressed proteins ($P<0.05$) were visually represented using bubble plots, revealing pathways related to collagen-containing extracellular matrix, oxygen level response, lipid metabolic process regulation, hypoxia response, decreased oxygen level response, drug response, lysosomal membrane, lytic vacuole membrane, vacuolar membrane, IL-1 response, intracellular lipid transport, collagen trimer, blood microparticles, intracellular lipid and sterol transport regulation, low-density lipoprotein particle receptor catabolic process regulation, and the estrous cycle (*Figure 10D*). However, post-CC16 intervention, a limited set of genes including *ETS1*, *ZBTB38*, *PSMD2*, *EIF3A*, *FuUS*, and *C15orf52* were observed to be downregulated (*Figure 10E*). ETS1 was selected for further validation through Western blot analysis, confirming its upregulation by CC16 (*Figure 10F*).

Discussion

Exposure to elevated levels of $PM_{2.5}$ has been identified as a risk factor for the exacerbation of asthma (16). Nevertheless, prior research has failed to conclusively elucidate the intricate relationship between $PM_{2.5}$ and the underlying mechanisms that trigger acute asthmatic episodes. Our findings indicate that exposure to $PM_{2.5}$ can result in respiratory acidosis, augmented airway resistance, damage to lung tissue, inflammatory responses, and dysfunction of the airway epithelium. Additionally, this exposure upregulates proteins associated with inflammation and pyroptosis (17). However, our study has revealed that CC16 possesses the capability to mitigate this pathological damage by down-regulating these inflammatory and pyroptosis-related proteins. A pivotal discovery of this research is the mechanistic protection offered by CC16 against lung damage induced by $PM_{2.5}$, suggesting the potential for CC16-based therapeutic interventions in the prevention of asthma exacerbation.

$PM_{2.5}$ are minute enough to penetrate into the distal airways, thereby posing a threat to the respiratory system (18). A growing body of research indicates that $PM_{2.5}$ can precipitate diverse forms of cellular demise, including autophagy, necrosis, apoptosis, pyroptosis, and

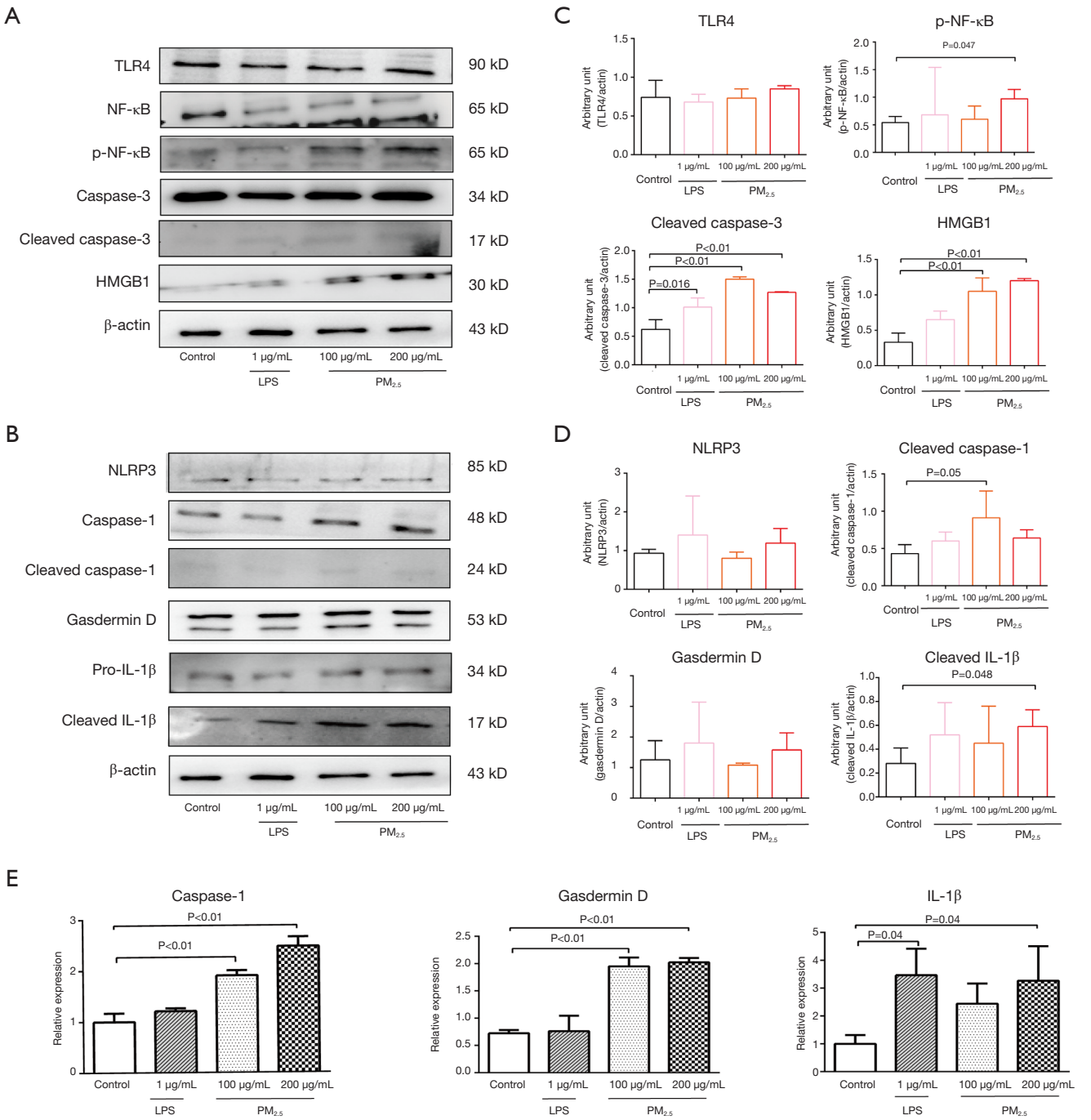

Figure 7 Western blot and RNA analysis of inflammatory and pyroptosis signaling pathways in BEAS-2B cells. (A-D) Western blot. (E) RNA analysis. Full-length blots/gels were presented in Figure S3. TLR4, toll-like receptor 4; NF-κB, nuclear factor-κB; p-, phospho-; HMGB1, high mobility group box 1; LPS, lipopolysaccharide; $PM_{2.5}$, particulate matter 2.5; NLRP3, nucleotide-binding oligomerization domain-like receptor family pyrin domain containing 3; IL-1β, interleukin-1β.

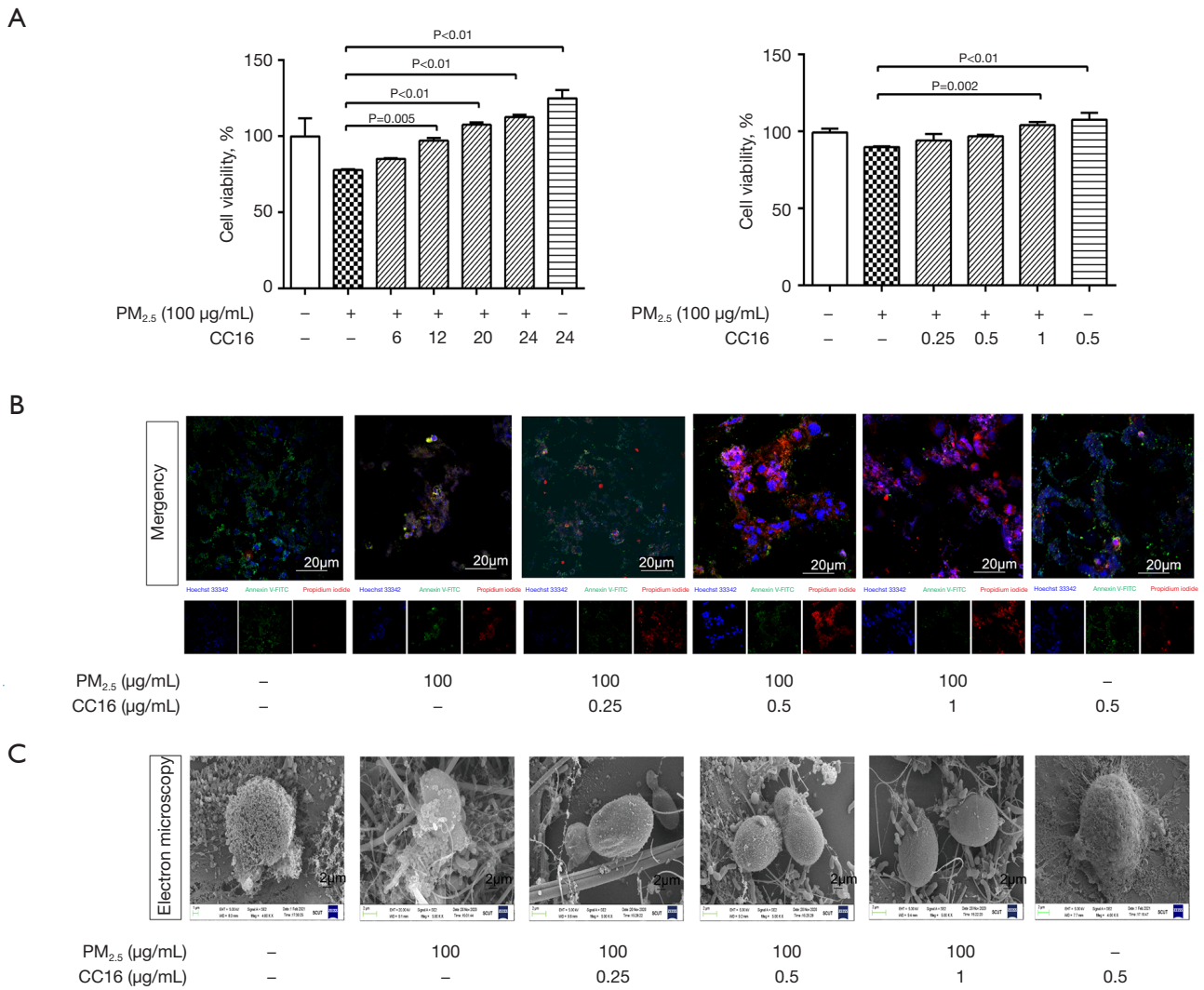

Figure 8 Light microscopy, CCK-8 analysis, confocal microscopy, and electron microscopy to determine the viability of BEAS-2B cells treated with CC16. (A) Cell viability was inferred from CCK-8 analysis. (B) Confocal microscopy, Hoechst 33342 staining (blue), Annexin V-FITC (green), PI (red). (C) Electron microscopy. $PM_{2.5}$, particulate matter 2.5; CC16, club cell secretory protein 16; EHT, electron high tension; WD, working distance; Mag, magnification; SCUT, South China University of Technology; CCK-8, Cell Counting Kit-8; FITC, fluorescein isothiocyanate; PI, propidium iodide.

ferroptosis (19,20). Our prior comprehensive *in vivo* and *in vitro* analyses have revealed that $PM_{2.5}$-induced asthma encompasses the involvement of pyroptosis-related proteins, namely NLRP3, caspase-1, gasdermin D, and IL-1β. This pyroptotic process is initiated through the canonical inflammasome pathway, which orchestrates the recruitment and activation of caspase-1 (21). Subsequently, caspase-1 processes and activates IL-18 and IL-1β, which are inflammatory mediators that truncate the N-terminal sequence of gasdermin D, prompting its membrane association and pore formation, ultimately culminating in cellular pyroptosis (22,23). Furthermore, studies conducted by Wang *et al.* and Huang *et al.* have demonstrated that $PM_{2.5}$ elicits lung toxicity via the suppression of NLRP3 inflammasome-mediated pyroptosis (24,25). Additionally, Xiong *et al.* have reported that the ablation of the pyroptosis-associated protein NLRP3 in macrophages has the potential to mitigate pyroptosis and $PM_{2.5}$-induced lung

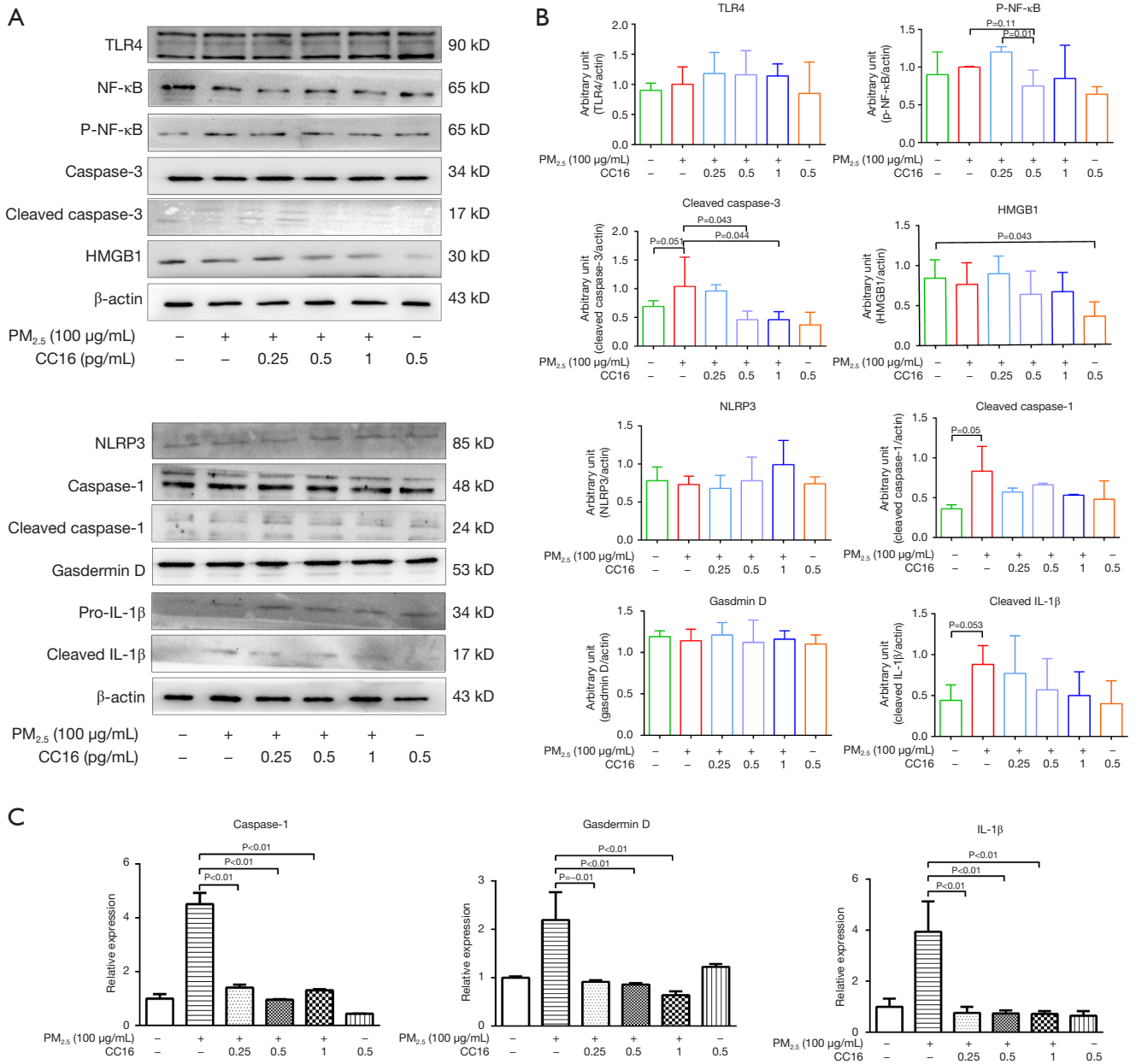

Figure 9 Western blot and PCR analysis of inflammatory and pyroptosis signaling pathways after CC16 treatment in BEAS-2B cells. (A,B) Western blot. (C) RNA analysis. Full-length blots/gels were presented in Figure S4. TLR4, toll-like receptor 4; NF-κB, nuclear factor-κB; p-, phospho-; HMGB1, high mobility group box 1; $PM_{2.5}$, particulate matter 2.5; CC16, club cell secretory protein 16; NLRP3, nucleotide-binding oligomerization domain-like receptor family pyrin domain containing 3; IL-1β, interleukin-1β; PCR, polymerase chain reaction.

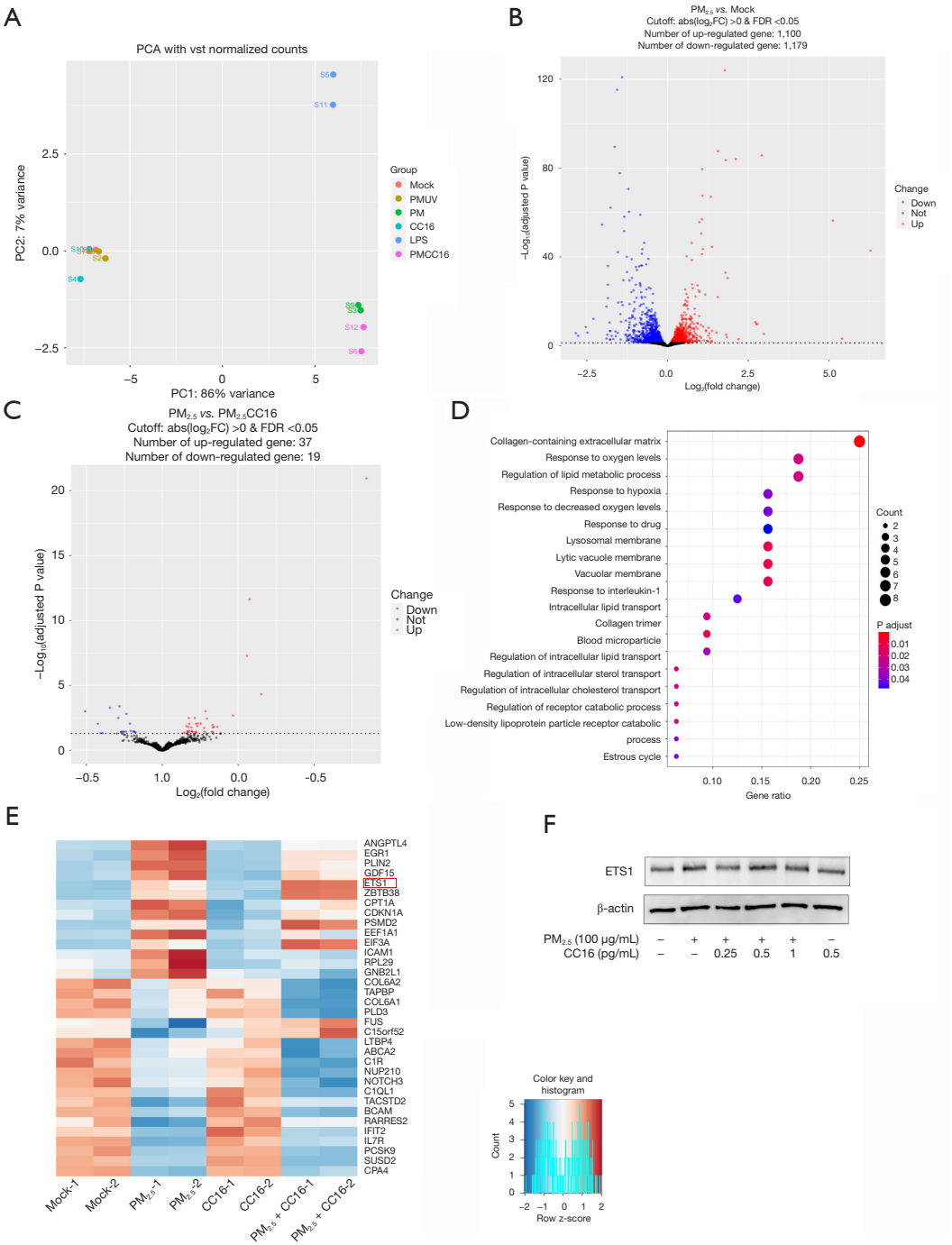

Figure 10 The intervention of CC16 on AECs pyroptosis following exposure to $PM_{2.5}$ utilizing transcriptome analysis in BEAS-2B cells. (A) PCA. (B) Two volcano plots display differential genes between the $PM_{2.5}$ and control groups. (C) Two volcano plots display differential genes between the CC16 group and the $PM_{2.5}$ group. (D) GO analysis investigates the pathophysiological process involved in the intervention of CC16. (E) Heat map of differential gene expression induced by CC16 intervention. (F) Western blot validation was performed on ETS1 of $PM_{2.5}$ exposed-AEC pyroptosis induced by CC16 intervention. Full-length blots/gels were presented in Figure S5. PCA, principal component analysis; PC, principal component; PMUV, $PM_{2.5}$ + ultraviolet; PM, particulate matter; CC16, club cell secretory protein 16; LPS, lipopolysaccharide; PMCC16, $PM_{2.5}$ + CC16; $PM_{2.5}$, particulate matter 2.5; FC, fold change; FDR, false discovery rate; ETS1, E26 transformation-specific homolog 1; AEC, airway epithelial cell; GO, Gene Ontology.

toxicity (26).

The risk of asthma is exacerbated by the connection between low CC16 levels and more frequent asthma symptoms, indicative of a dose-response relationship (27,28). Additionally, a study discovered that reduced CC16 mRNA expression in bronchial epithelial cells is associated with the severity of asthma (29). Recently, CC16 has been extensively investigated, with a focus on its regulatory role in inflammatory pathways within immune cells (30). Pang *et al.* demonstrated that recombinant CC16 inhibits the production of TNF-α, IL-6, and IL-8 in LPS-treated RAW264.7 cells (31). Furthermore, CC16 has been reported to suppress NF-κB nuclear translocation and matrix metalloprotein 9 production in LPS-stimulated rat tracheal epithelial cells (32). In sepsis-induced ALI, Janicova *et al.* observed that endogenous CC16 functions as an intrinsic anti-inflammatory signal, modulating early macrophage-driven inflammation. In a study examining particle-induced inflammation (33). Cui *et al.* found that CC16 significantly reduced IL-1β, TNF-α, and IL-6 protein and mRNA levels in THP-1 macrophages (34). They also showed that CC16 mitigated the elevation of pro-IL-1β, NLRP3, and caspase-1 levels induced by silica particle exposure. Our research reveals that CC16 repairs airway epithelial proteins by targeting signal proteins associated with pyroptosis and inflammation, thereby promoting cell proliferation. This dual functionality and mechanism of action underscores the potential for further investigation into the role of CC16 in airway epithelial repair.

Our previous experimental results have conclusively shown that CC16 exerts its inhibitory effect on LPS-stimulated apoptosis by activating the PI3K/AKT/mTOR/ERK1/2 signaling cascade, while simultaneously inhibiting the release of inflammatory factors by deactivating the TLR4/NF-κB signaling pathway. In the current study, we have uncovered that $PM_{2.5}$-induced pyroptosis involves the deactivation of the NLRP3/caspase-1 signaling pathway and an up-regulation of inflammatory mediator expression, which is mediated through the inhibition of the TLR4/NF-κB/MAPK/caspase-3 signaling pathway. Notably, both of these processes are simultaneously mitigated by CC16. In particular, CC16 exhibits a high degree of specificity towards HMGB1. Our cellular and animal models have demonstrated that CC16 is capable of inhibiting the $PM_{2.5}$-induced release of HMGB1. Liu *et al.* have documented that CC16 alleviates airway inflammation and damage mediated by house dust mites by suppressing AEC apoptosis in an HMGB1-dependent manner (35). Additionally, Huang *et al.* have identified that HMGB1, in synergy with IL-1β, can promote the dysfunction of the epithelial barrier (36). However, the fundamental mechanism underlying how CC16 inhibits HMGB1 and IL-1β remains to be further elucidated. Based on the transcriptome analysis, it has been observed that CC16 up-regulate genes associated with cellular proliferation and repair processes, such as ETS1 exhibits a close association with the AKT/mTOR proliferation pathway and exerts regulatory control over the downstream NF-κB signaling (37).

However, it is imperative to acknowledge several constraints inherent in our study. Firstly, substantial advancements in conceptual understanding are crucial, with a particular emphasis on refining the experimental framework utilized for the animal model. In order to definitively ascertain whether CC16 modulates anaphylactic inflammation within asthmatic airways or exerts influence on $PM_{2.5}$-induced inflammation, it is advisable to incorporate four distinct control groups: control + OVA, control + OVA + CC16, control + $PM_{2.5}$, and control + $PM_{2.5}$ + CC16. Dr. Wang Aili, an esteemed member of our research team, has augmented the control group composition in accordance with this experimental blueprint, subsequently validating CC16's reparative capabilities in response to injuries stemming from both $PM_{2.5}$ and OVA. The imminent publication of her article is highly anticipated. Furthermore, it is advisable to embark on a new study specifically tailored to explore the intricate relationship between asthma and $PM_{2.5}$. This will involve conducting an additional animal experiment, incorporating the aforementioned control groups. Nevertheless, the paucity of supporting evidence hinders the assertion of a significant difference in sRAW between asthma and the negative control. Nonetheless, the data gathered from HE, arterial blood gas analysis, and IL-1β levels in BAL provides robust evidence for the successful establishment of the asthma model. In future studies, it is necessary to address the confounding effects arising from the increased expression of inflammatory and pyroptotic signals in lung structural cells, as opposed to infiltrating leukocytes, by employing techniques such as immunohistochemistry or flow cytometry. Additionally, the reviewer noted that a significant rise in $PaCO_2$ often signals impending respiratory failure. We think this may be linked to prolonged OVA-induced airway spasms, arterial blood gas sampling methods, and possible use of pentobarbital. Future researchers should consider this.

Conclusions

To summarize, CC16 exhibits the capability to mitigate $PM_{2.5}$-mediated airway epithelial injury by modulating the inflammatory cascade and pyroptotic processes. These observations underscore the potential of CC16 as a therapeutic approach for reducing health hazards stemming from $PM_{2.5}$ exposure in asthmatic individuals.

Acknowledgments

We thank all investigators for their excellent assistance in this research. Pulmonary function test was undertaken by Xiu Yu and Hongchang Chen (Institute of Respiratory Diseases, Shenzhen People's Hospital). We wish to thank Xinhui Bi (Institute of Geochemistry, Chinese Academy of Sciences), Qi Fan and Shenxun Zhou (Sun Yat-sen University) for collecting, Xinzhi Bi (Guangzhou Institute of Geographical Chemistry) for analyzing $PM_{2.5}$, as well as Jiajie Shan and Jian Wang (School of Medicine, Southern China University of Technology) for their technical assistance. We thank to the language editor of Abdelouahab Bellou. The authors declare that artificial intelligence is not used in this study.

Footnote

Reporting Checklist: The authors have completed the ARRIVE reporting checklist. Available at https://jtd.amegroups.com/article/view/10.21037/jtd-24-1371/rc

Data Sharing Statement: Available at https://jtd.amegroups.com/article/view/10.21037/jtd-24-1371/dss

Peer Review File: Available at https://jtd.amegroups.com/article/view/10.21037/jtd-24-1371/prf

Funding: The research was funded by National Natural Science Foundation of China (No. 81970012 to J.W.), the Natural Science Foundation of Guangdong Province (No. 2023A1515011587 to J.W.), the Project of Guangdong Provincial Department of Finance (No. KS0120220270 to J.W.), the Key R&D Projects of Guangdong Provincial Science and Technology Plan (No. 2109B020227006 to J.W.), the National Natural Science Fund of China (No. 82302462 to J.L.), the Guang Dong Basic and Applied Basic Research Foundation (No. 2022A1515111206 to J.L.), the Guangdong Provincial Medical Science and Technology Research Fund Project (No. 20221115145253272 to J.L.), the Shenzhen Key Medical Discipline Construction Fund (No. SZXK047 to J.L.), the High-Level Medical Team of Shenzhen "Three Famous Medical and Health Project", the Key Laboratory of Emergency and Trauma (Hainan Medical University), Ministry of Education (No. KLET-202220 to J.L.), and the Science and Technology Planning Project of Shenzen Municipality (No. YJ20230807140904010 to J.L.).

Conflicts of Interest: All authors have completed the ICMJE uniform disclosure form (available at https://jtd.amegroups.com/article/view/10.21037/jtd-24-1371/coif). The authors have no conflicts of interest to declare.

Ethical Statement: The authors are accountable for all aspects of the work in ensuring that questions related to the accuracy or integrity of any part of the work are appropriately investigated and resolved. The study was conducted in accordance with the Guidelines for the Care and Use of Laboratory Animals issued by the Ministry of Science and Technology of the People's Republic of China (the National Standard GB/T 35892-2018). The research was approved by the Ethics Committee of Southern Medical University (approval No. BYL20231202).

References

1. Zhang L, Wilson JP, MacDonald B, et al. The changing PM2.5 dynamics of global megacities based on long-term remotely sensed observations. Environ Int 2020;142:105862.
2. Wang Y, Duan X, Wang L. Spatial-Temporal Evolution of PM2.5 Concentration and its Socioeconomic Influence Factors in Chinese Cities in 2014;2017. Int J Environ Res Public Health 2019;16:985.
3. Wei H, Yuan W, Yu H, et al. Cytotoxicity induced by fine particulate matter (PM(2.5)) via mitochondria-mediated apoptosis pathway in rat alveolar macrophages. Environ

Sci Pollut Res Int 2021;28:25819-29.
4. Frey A, Lunding LP, Ehlers JC, et al. More Than Just a Barrier: The Immune Functions of the Airway Epithelium in Asthma Pathogenesis. Front Immunol 2020;11:761.
5. Bonser LR, Erle DJ. The airway epithelium in asthma. Adv Immunol 2019;142:1-34.
6. Gurgone D, McShane L, McSharry C, et al. Cytokines at the Interplay Between Asthma and Atherosclerosis? Front Pharmacol 2020;11:166.
7. Kim RY, Pinkerton JW, Essilfie AT, et al. Role for NLRP3 Inflammasome-mediated, IL-1β-Dependent Responses in Severe, Steroid-Resistant Asthma. Am J Respir Crit Care Med 2017;196:283-97.
8. Almuntashiri S, Zhu Y, Han Y, et al. Club Cell Secreted Protein CC16: Potential Applications in Prognosis and Therapy for Pulmonary Diseases. J Clin Med 2020;9:4039.
9. Mukherjee AB, Zhang Z, Chilton BS. Uteroglobin: a steroid-inducible immunomodulatory protein that founded the Secretoglobin superfamily. Endocr Rev 2007;28:707-25.
10. Lin J, Zhang W, Wang L, et al. Diagnostic and prognostic values of Club cell protein 16 (CC16) in critical care patients with acute respiratory distress syndrome. J Clin Lab Anal 2018;32:e22262.
11. Lin J, Li J, Shu M, et al. The rCC16 Protein Protects Against LPS-Induced Cell Apoptosis and Inflammatory Responses in Human Lung Pneumocytes. Front Pharmacol 2020;11:1060.
12. Han Y, Zhu Y, Almuntashiri S, et al. Extracellular vesicle-encapsulated CC16 as novel nanotherapeutics for treatment of acute lung injury. Mol Ther 2023;31:1346-64.
13. Guerra S, Vasquez MM, Spangenberg A, et al. Club cell secretory protein in serum and bronchoalveolar lavage of patients with asthma. J Allergy Clin Immunol 2016;138:932-934.e1.
14. Taniguchi N, Konno S, Hattori T, et al. The CC16 A38G polymorphism is associated with asymptomatic airway hyper-responsiveness and development of late-onset asthma. Ann Allergy Asthma Immunol 2013;111:376-381.e1.
15. Percie du Sert N, Hurst V, Ahluwalia A, et al. The ARRIVE guidelines 2.0: updated guidelines for reporting animal research. BMJ Open Sci 2020;4:e100115.
16. Wang YY, Liu XL, Zhao R. Induction of Pyroptosis and Its Implications in Cancer Management. Front Oncol 2019;9:971.
17. Liu X, Li Z, Shan J, et al. PM(2.5) Exposure Inhibits Transepithelial Anion Short-circuit Current by Downregulating P2Y2 Receptor/CFTR Pathway. Int J Med Sci 2024;21:1929-44.
18. Liu G, Li Y, Zhou J, et al. PM2.5 deregulated microRNA and inflammatory microenvironment in lung injury. Environ Toxicol Pharmacol 2022;91:103832.
19. Li R, Zhou R, Zhang J. Function of PM2.5 in the pathogenesis of lung cancer and chronic airway inflammatory diseases. Oncol Lett 2018;15:7506-14.
20. Wang Y, Zhong Y, Liao J, et al. PM2.5-related cell death patterns. Int J Med Sci 2021;18:1024-9.
21. Chen X, Wang F, Lin J, et al. The consistently up-regulated expression of NLRP3 in severe asthma patients from mRNA microarray and ovalbumin-induced mouse model of asthma. J Thorac Dis 2024;16:4957-66.
22. Vasudevan SO, Behl B, Rathinam VA. Pyroptosis-induced inflammation and tissue damage. Semin Immunol 2023;69:101781.
23. Man SM, Karki R, Kanneganti TD. Molecular mechanisms and functions of pyroptosis, inflammatory caspases and inflammasomes in infectious diseases. Immunol Rev 2017;277:61-75.
24. Wang Y, Duan H, Zhang J, et al. YAP1 protects against PM2.5-induced lung toxicity by suppressing pyroptosis and ferroptosis. Ecotoxicol Environ Saf 2023;253:114708.
25. Huang D, Shen Z, Zhao S, et al. Sipeimine attenuates PM2.5-induced lung toxicity via suppression of NLRP3 inflammasome-mediated pyroptosis through activation of the PI3K/AKT pathway. Chem Biol Interact 2023;376:110448.
26. Xiong R, Jiang W, Li N, et al. PM2.5-induced lung injury is attenuated in macrophage-specific NLRP3 deficient mice. Ecotoxicol Environ Saf 2021;221:112433.
27. Voraphani N, Stern DA, Ledford JG, et al. Circulating CC16 and Asthma: A Population-based, Multicohort Study from Early Childhood through Adult Life. Am J Respir Crit Care Med 2023;208:758-69.
28. Bernard A, Marchandise FX, Depelchin S, et al. Clara cell protein in serum and bronchoalveolar lavage. Eur Respir J 1992;5:1231-8.
29. Li X, Guerra S, Ledford JG, et al. Low CC16 mRNA Expression Levels in Bronchial Epithelial Cells Are Associated with Asthma Severity. Am J Respir Crit Care Med 2023;207:438-51.
30. Xu B, Janicova A, Vollrath JT, et al. Club cell protein 16 in sera from trauma patients modulates neutrophil migration and functionality via CXCR1 and CXCR2. Mol Med 2019;25:45.
31. Pang M, Wang H, Bai JZ, et al. Recombinant rat CC16

protein inhibits LPS-induced MMP-9 expression via NF-κB pathway in rat tracheal epithelial cells. Exp Biol Med (Maywood) 2015;240:1266-78.
32. Pang M, Yuan Y, Wang D, et al. Recombinant CC16 protein inhibits the production of pro-inflammatory cytokines via NF-κB and p38 MAPK pathways in LPS-activated RAW264.7 macrophages. Acta Biochim Biophys Sin (Shanghai) 2017;49:435-43.
33. Janicova A, Becker N, Xu B, et al. Endogenous Uteroglobin as Intrinsic Anti-inflammatory Signal Modulates Monocyte and Macrophage Subsets Distribution Upon Sepsis Induced Lung Injury. Front Immunol 2019;10:2276.
34. Cui X, Xu R, Zhang H, et al. Exogenous Clara cell protein 16 attenuates silica particles-induced inflammation in THP-1 macrophages by down-regulating NF-κB and caspase-1 activation. J Toxicol Sci 2020;45:651-60.
35. Liu M, Lu J, Zhang Q, et al. Clara cell 16 KDa protein mitigates house dust mite-induced airway inflammation and damage via regulating airway epithelial cell apoptosis in a manner dependent on HMGB1-mediated signaling inhibition. Mol Med 2021;27:11.
36. Huang W, Zhao H, Dong H, et al. High-mobility group box 1 impairs airway epithelial barrier function through the activation of the RAGE/ERK pathway. Int J Mol Med 2016;37:1189-98.
37. Chen YC, Chuang TY, Liu CW, et al. Particulate matters increase epithelial-mesenchymal transition and lung fibrosis through the ETS-1/NF-κB-dependent pathway in lung epithelial cells. Part Fibre Toxicol 2020;17:41.

Cite this article as: Lin J, Chen X, Chen Y, Zeng X, Wang F, Luo S, Jiang L, Hu W, Liu X, Zhang J, Wu J. Club cell secretory protein 16 promotes cell proliferation and inhibits inflammation and pyroptosis in response to particulate matter 2.5-induced epithelial damage in asthmatic mice. J Thorac Dis 2025;17(2):753-773. doi: 10.21037/jtd-24-1371